Electron Delocalization in Isocyanates, Formamides, and Ureas: Importance of Orbital Interactions

Prasad V. Bharatam,*,† Rajnish Moudgil, and Damanjit Kaur

Department of Chemistry, Guru Nanak Dev University, Amritsar-143 005, India

Received: September 21, 2002; In Final Form: December 19, 2002

The electron delocalization in isocyanates, amides, and ureas has been studied using ab initio MO and density functional methods. The observed trends in the C—N rotational barriers and N-inversion barriers in these systems have been explained in terms of orbital interactions. NBO analysis indicates that there is $n_N \rightarrow \pi^*_{[C-X]}$ electron delocalization in amides, which increases with a decrease in the energy difference (ΔE) between the two interacting orbitals. This phenomenon, rather than electronegativity, is responsible for the observed increase in the C—N rotational barrier in amides X═C(R)—NH_2 (R = H, NH_2) in the order X = O < S < Se.

Introduction

According to the resonance model proposed by Pauling,[1] the electron delocalization should increase with an increase in the electronegativity of X in X═C(H)—NH_2.[2] The resonance in these systems can be represented as in Scheme 1. Contribution from the resonance forms **1**−**3** have been expected to be important in the electronic description of amides; however, with a decrease in the electronegativity of X, contribution from resonance form **3** is expected to reduce. Accordingly, selenocarbonyl systems should have weaker electron delocalization relative to their O and S counterparts. However, the experimental and theoretical observations point to the contrary. Wiberg and co-workers have studied this problem in thioamides by performing ab initio calculations, using density difference maps, and concluded that the charge polarization in C—S bond is much weaker than that in the C═O bond and hence the contribution from resonance structure **2** is much more reduced in thioformamide relative that in formamide.[3] Glendening and Hrabal studied the problem using natural resonance theory and concluded that the weight of the dipolar form **3** increases from formamide to telluroformamide and showed that polarizability of the C—X bond rather than the electronegativity of X plays important role in allowing the chalcogen to accommodate more charge density.[4] On the basis of integrated Fermi correlation Ladig and Camaron showed that the thioamides should be viewed as special cases of amines.[2] Lauvergnat and Hiberty, employing valence bond theory, showed that resonance stabilization does not wholly account for the C═N bond rotational barriers and the preference of the nitrogen lone pair to stay perpendicular to the molecular plane also should be considered.[5] Wiberg and Rush reported that solvent effects are larger on the rotational barrier of a thioamide relative to that in an amide because of a larger dipole moment.[3] Wiberg and Rush[3a] as well as Lauvergnat and Hiberty pointed out that the greater charge transfer from N to S in thioamides in comparison to the charge transfer from N to O in amides is responsible for the greater electron delocalization in thioamides. The above cited work clearly indicates that several factors control the resonance in the systems with the general formula X═C(R)—NH_2 and calls for further work.

SCHEME 1

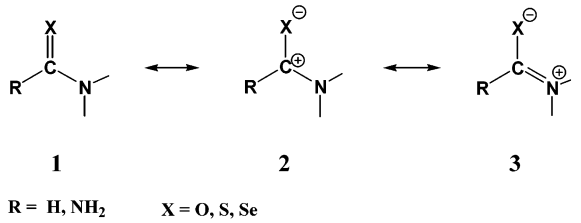

In this paper we present studies on the electron delocalization in isocyanates (X═C═NH), formamides (X═C(H)—NH_2), and ureas (X═C(NH_2)$_2$), where X is a chalcogen (O or S or Se). Second-order electronic interactions have been quantitatively estimated using the natural bond orbital method (NBO). Our results indicate that negative hyperconjugation also plays an important role in the C—N rotational process apart from delocalization, and the energy difference between $\pi^*_{(C-X)}$ and $n_{(N)}$ plays an important role in deciding the extent of electron delocalization. The details are given below.

Computational Details

Ab initio MO[6] and density functional (DFT)[7] calculations have been carried out using the GAUSSIAN98W package,[8] the windows version of the GAUSSIAN98 suite of programs. Complete optimizations have been performed on isocyanates, (**io-1**, **it-1**, **is-1**), formamides (**f-1**, **tf-1**, **sf-1**), and ureas (**u-1**, **tu-1**, **su-1**) using HF, MP2(full),[9] B3LYP,[10] and B3PW91[11] methods and the 6-31+G* basis set. Complete optimizations have also been performed on the N inversion, C—N rotational isomers, and transition states of the above systems using the same methods. Frequencies were computed analytically for all optimized species at all levels (except MP2(full)) to characterize each stationary point as a minimum or a transition state and to determine the zero point vibrational energies (ZPE). The calculated ZPE values have been scaled by a factor of 0.9153, 0.9806, and 0.9772 for HF, B3LYP, and B3PW91 levels, respectively.[12] To obtain more accurate estimates of C—N rotational barriers and N-inversion barriers, calculations have

† Current address: Department of Medicinal Chemistry, National Institute of Pharmaceutical Education and Research (NIPER), S.A.S. Nagar (Mohali), 160 062 Punjab, India. E-mail: bharatam@glide.net.in.

10.1021/jp027044+ CCC: $25.00
Published on Web 02/06/2003

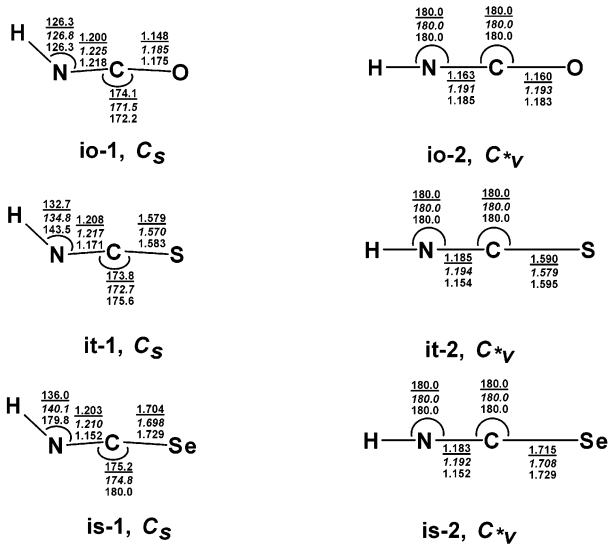

Figure 1. Important geometeric parameters at three levels (viz. HF/6-31+G*, MP2(full)/6-31+G*, and B3LYP/6-31+G*) of isocyanate, isothiocyanate, and isoselenocyanate and their corresponding linear structure. Distances are in ångstroms and angles are in degrees.

been repeated at the G2 level also.[13] Atomic charges in all the structures were obtained using the natural population analysis (NPA) method within the natural bond orbital (NBO) approach[14] with the MP2 densities using the MP2(full)/6-31+G* wave function. NBO analysis has been used to quantitatively estimate the second-order energy interactions ($E^{(2)}$ ($=-2F_{ij}/\Delta E_{ij}$) energy due to second-order interaction ($E_{ij} = E_i - E_j$ is energy difference between the interacting molecular orbitals i and j; F_{ij} is the Fock matrix element for the interaction between i and j). To obtain the supportive arguments on the observed trends in the electron delocalization, MP2(full)/6-31+G* optimizations and NBO analysis on the corresponding structure have been carried out on $X{=}C(R)NH_2$ systems (with X = CH_2, NH, PH, AsH; R = H, NH_2) also. In the discussion the geometric parameters obtained using the MP2(full)/6-31+G* level and energies obtained using the G2 method are employed until otherwise specifically mentioned.

Results and Discussion

Isocyanates. The experimentally evaluated C—N—H angle in isoselenocynate (Se═C═N—H, 143.0°) is larger than that in isothiocyanate (S═C═N—H, 131.7°) and isocyanate (O═C═N—H, 123.9°). Similarly, the C—N—Me angle in methylisoselenocyanate (Se═C═N—Me)[15a] (157.0°)[15b,c] has been shown to be larger than that in methylisothiocyanate (147.5°)[15c] and in methylisocyanates (140.0°).[15b,d] The gradual increase in the C—N—R angles in the above systems can be attributed to the increase in the electron delocalization in the order O < S < Se. In this section, we report the results of theoretical calculations on **io-1**, **it-1**, and **is-1** (Figure 1) and quantitatively estimate the electron delocalizations in them using the NBO method. Complete optimizations show that **io-1**, **it-1**, and **is-1** have C_s symmetric arrangement. The calculated C—N—H angles (Figure 1) are much larger than the sp^2 angle (120.0°). The calculated C—N—H angles (MP2(full) method) are very comparable to the experimental estimates and show a gradual increase in the order O (126.3°) < S (134.8°) < Se (140.0°).[15e] These data and similar trends in MeNCX (X = O, S, Se) indicate that Se systems show stronger delocalization. The C—N bond distance in these systems is smaller than the C═N double bond length in $H_2C{=}NH$ (1.284 Å) and show a gradual decrease in the order O (1.225) > S (1.217) > Se (1.209 Å). During the N-linearization process, the C—N bond contraction decreases in the order **io** (0.035 Å) > **it** (0.023 Å) > **is** (0.018 Å) (Table 1). This indicates that the partial triple bond character and hence the zwitterionic character in these systems increase in the order O < S < Se. These geometrical data can be rationalized only when we consider that there is a strong delocalization of lone pair electrons on nitrogen onto the π frame of isocyanates and that the electron delocalization increases with an increase in the size of X. The strong electron delocalization in isocyanates should reduce the N-inversion barrier. The calculated linearization energies in **io-1**, **it-1**, and **is-1** are in the decreasing order 4.96 > 2.36 > 2.04 kcal/mol (Table 3), respectively, at the G2 level,[15h] much smaller than the N-inversion barrier in $H_2C{=}$NH (30.1 and 28.0 kcal/mol at the same levels).

TABLE 1: C—N and C—X Distances and Variation in Them (Å) at MP2(full)/6-31+G*

structure		C—N	C—N variation	C—X	C—X variation
isocyanate	**io**	1.225	0.035[a]	1.185	0.008[b]
isothiocyanate	**it**	1.217	0.023[a]	1.570	0.009[b]
isoselenocyanate	**is**	1.209	0.017[a]	1.698	0.010[b]
formamide	**f**	1.360	0.079[c]	1.228	0.009[d]
thioformamide	**tf**	1.350	0.087[c]	1.634	0.015[d]
selenoformamide	**sf**	1.346	0.087[c]	1.764	0.016[d]
urea	**u**	1.388	0.061[c]	1.229	0.000[d]
thiourea	**tu**	1.374	0.070[c]	1.650	0.006[d]
selenourea	**su**	1.367	0.077[c]	1.787	0.010[d]

[a] C—N bond contraction as a function of N linearization. [b] C—X bond elongation as a function of N linearization. [c] C—N bond elongation as a function of C—N rotation. [d] C—X bond contraction as a function of C—N rotation.

TABLE 2: C—N—H linearization Energies (kcal/mol, ZPE Corrected Values) of Isocyanate (io), Isothiocyanate (it), and Isoselenocyanate (is) Obtained Using Different Theoretical Methods

level	isocyanate	isothiocyanate	isoselenocyanate
HF/6-31+G*	3.67	0.00	0.00
MP2/6-31+G*	4.66	2.87	1.07
MP2(fu)/6-31+G*	4.41	2.69	0.93
B3LYP/6-31+G*	4.29	2.55	1.20
B3PW91/6-31+G*	4.28	2.54	1.20
G2	4.95	2.36	2.04

NBO analysis shows that the occupancies of the nitrogen lone pair in **io-1**, **it-1**, and **is-1**, respectively, are only 1.755, 1.686, and 1.648 e; i.e., a significant amount of electron density of the lone pair on N is involved in the delocalization. The energy $E^{(2)}$ for the $n_N \rightarrow \pi^*_{C-X}$ delocalization in **io-1**, **it-1**, and **is-1**, respectively, are 47.35, 50.56, and 43.51 kcal/mol (Table 3). Isocyanates are also characterized by $n_N \rightarrow \sigma^*_{C-X}$ electron delocalization (negative hyperconjugation), with $E^{(2)}$ values of 24.22, 23.15, and 30.80 kcal/mol in **io-1**, **is-1**, and **it-1**, respectively. The sum of these two $E^{(2)}$ values accounts for the energy due to N lone pair electron delocalization. NBO analysis indicates that the occupancy of the lone pair on the nitrogen in isocyanates decreases in the same order O (1.755) > S (1.686) > Se (1.648 e) (Table 3) and negative charge localization on the NH group is also reduced in the same order O (−0.434) > S (−0.302) > Se (−0.291) (Table 3). The total second-order energy due to N lone pair delocalization (i.e., sum of the second-order energy due to $n_N \rightarrow \pi^*_{C-Se}$ and $n_N \rightarrow \sigma^*_{C-Se}$ interactions) increases in the order **io-1** (71.51) < **it-1** (73.71) < **is-1** (74.31 kcal/mol).

TABLE 3: NBO Analysis of Isocyanate (io), Isothiocyanate (it), and Isoselenocyanate (is) at the MP2(full)/6-31+G* Level

		second-order interactions			occupancy	charges		
compound	interaction	$E^{(2)}$ [a]	$E_j - E_i$ [b]	F_{ij} [b]	$\rho_{n(N)}$	X	C	NH
io-1	$n_{N3}-\pi^*_{C-O}$	47.35	0.82	0.177	1.755	−0.617	1.050	−0.434
	$n_N-\sigma^*_{C-O}$	24.22	1.39	0.172				
it-1	$n_{N3}-\pi^*_{C-S}$	50.56	0.66	0.163	1.686	−0.031	0.339	−0.308
	$n_N-\sigma^*_{C-S}$	23.15	0.89	0.143				
is-1	$n_{N3}-\pi^*_{C-Se}$	43.51	0.62	0.148	1.648	0.00	0.291	−0.291
	$n_N-\sigma^*_{C-Se}$	30.80	0.82	0.149				

[a] In kcal/mol. [b] In au.

The electronic structure of isoselenocyanate can be compared to that of linear ketenimines **A**, which have been shown to exist in zwitterionic state **B**.[16] The partial linearity in **is-1** indicates

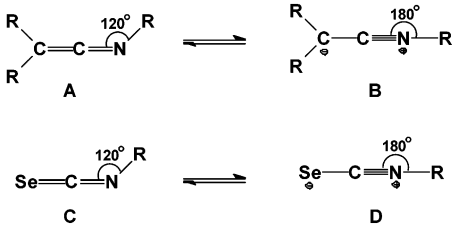

that the resonance between the two structures **C** and **D** should be taken as the electronic structure of **is-1**. It was reported that the contribution from structure **B** increases in ketenimines with the electron donating capacity of the R group.[13] Correspondingly, Se=C=N−Me should have stronger zwitterionic character with a larger C−N−Me angle. MP2(full)/6-31+G* calculations predict a C−N−Me angle of 172.8° for Se=C=NMe. Though this value is much higher than the experimentally reported C−N−Me angles (157.0° and 161.7°),[15a] the trends in the electron delocalization are in accordance with the expectations.

According to the resonance model, HNCO should have stronger electron delocalization among the three, because oxygen has a higher electronegativity. However, the above data and experimental observations indicate that electronegativity does not play an important role in the electron delocalization. The larger delocalization in the Se system can be attributed to the size of the X element to accommodate extra charge, as was suggested earlier. However, the charge on X and charge polarization along C−X bond are reduced in the order O > S > Se. NBO calculations show that the delocalization from the N lone pair increases from X = O to X = Se. This can be attributed to a strong decrease in the energy difference ($\Delta E_{ij} = E_i - E_j$) between the interacting molecular orbitals, because energy due to second-order interaction is inversely proportional to the ΔE_{ij}.[14] Though the Fock matrix element F_{ij} is also decreasing, the influence of the decrease in ΔE is very strong. Hence, it may be concluded that better orbital interactions due to the decreasing energy difference between interacting orbitals is mainly responsible for the increasing electron delocalization but not the electronegativity of X.

Formamides. The electronic structures of formamide, thioformamde, and selenoformamide have been reported earlier.[1−5,17] In this paper we report only a comparison of the electronic structures of formamide (**f-1**), thioformamide (**tf-1**), and selenoformamide (**sf-1**) (Figure 2). Thioformamide has been shown to have a higher electron delocalization relative to formamide because the C−N rotational barrier in **tf-1** is higher than that in **f-1**.[3b] Experimental estimates showed that the rotational barrier in thioformamide is larger than that in formamide.[18] Similarly, our earlier studies at the MP2/6-31+G* level

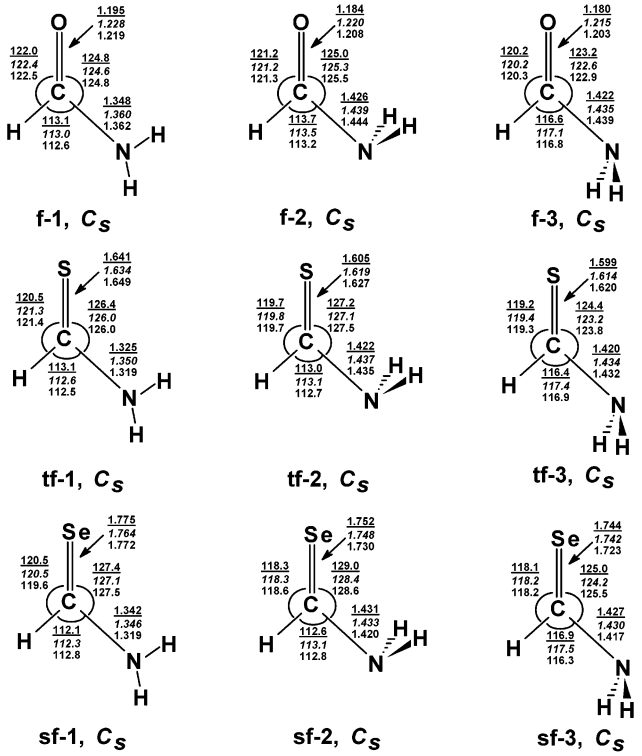

Figure 2. Different structures of formamide, thioformamide, and selenoformamide along with their important geometeric parameters at three levels (viz. HF/6-31+G*, MP(full)/6-31+G*, and B3LYP/6-31+G*. Distances are in ångstroms and angles are in degrees.

indicated that selenoformamide has a higher electron delocalization relative to **tf-1** and hence also to **f-1**.[18a] The C−N rotational barriers (Table 4) obtained at the G2 level in **f-1**, **tf-1**, and **sf-1** are in the order 15.97 < 18.02 < 19.72 kcal/mol, respectively. The calculated C−N rotational barriers in these systems account for two factors: (1) the energy rise due to breaking the partial pπ−pπ bond between carbon and nitrogen and (2) the energy gain due to the $n_N \rightarrow \sigma^*_{C-X}$ negative hyperconjugation (anomeric C−N π bond) in the rotational transition state. This can be clearly understood by studying the second-order delocalizations in selenoformamide. NBO analysis (Table 5) shows that the $n_N \rightarrow \pi^*_{C-Se}$ delocalization is very strong with a second-order interaction energy ∼120.4 kcal/mol. This strong delocalization is due to the small energy difference ΔE (0.45 au) and strong ($F_{ij} = 0.208$ au) between the interacting orbitals. In the rotational transition state **sf-2**, which has syn arrangement of Se−C−NH_2, the $n_N \rightarrow \pi^*_{C-Se}$ interaction disappears but $n_N \rightarrow \sigma^*_{C-Se}$ negative hyperconjugative interaction appears, with an $E^{(2)}$ of 12.87 kcal/mol (Table 5). This interaction induces an anomeric π character between C and N in **sf-2**.

The partial pπ−pπ C−N bond strength increases in the order **f-1** < **tf-1** < **sf-1** because the N lone pair delocalization in these systems follows the same order (Table 5). This is evidenced by

TABLE 4: Relative Energies (kcal/mol, ZPE Corrected Values) of Various Structures of Formamide (f), Thioformamide (tf), and Selenoformamide (sf) Obtained Using Different Theoretical Methods

structure	HF/6-31+G*	MP2/6-31+G*	MP2(full)/6-31+G*	B3LYP/6-31+G*	B3PW91/6-31+G*	G2
f-1	0.00	0.00	0.00	0.00	0.00	0.00
f-2	16.13	17.20	17.33	18.49	18.80	15.97
f-3	18.80	19.61	19.73	20.42	20.77	17.21
tf-1	0.00	0.00	0.00	0.00	0.00	0.00
tf-2	21.02	19.46	19.06	21.99	22.34	18.02
tf-3	23.09	21.06	21.19	23.82	24.25	19.15
sf-1	0.00	0.00	0.00	0.00	0.00	0.00
sf-2	22.77	20.70	20.89	22.73	23.03	18.60
sf-3	24.91	23.38	22.59	24.62	25.03	19.72

TABLE 5: NBO Analysis of Formamide (f), Thioformamide (tf), and Selenoformamide (sf) at the MP2(full)/6-31+G* Level

		second-order interaction			occupancy		charges			
compound	interaction	$E^{(2)}$ [a]	$E_i - E_j$	$F_{i,j}$	$\rho_{n(N)}$	$\rho_{\pi^*(C-O)}$	X	C	H	NH_2
f-1	$n_{N3}-\pi^*_{O1-C2}$	89.05	0.59	0.205	1.802	0.192	−0.724	0.661	0.147	−0.083
f-2	$n_{N3}-\sigma^*_{O1-C2}$	14.45	1.41	0.128	1.970	0.030	−0.633	0.658	0.158	−0.183
f-3	$n_{N3}-\sigma^*_{O1-C2}$	7.36	1.41	0.091	1.969	0.031	−0.599	0.943	0.137	−0.180
tf-1	$n_{N3}-\pi^*_{S1-C2}$	111.2	0.47	0.205	1.740	0.252	−0.204	−0.002	0.223	−0.007
tf-2	$n_{N3}-\sigma^*_{S1-C2}$	12.14	1.07	0.102	1.968	0.034	−0.018	−0.057	0.227	−0.152
tf-3	$n_{N3}-\sigma^*_{S1-C2}$	2.24	1.07	0.053	1.973	0.035	0.037	0.089	0.208	−0.157
sf-1	$n_{N3}-\pi^*_{Se1-C2}$	120.4	0.45	0.208	1.723	0.269	−0.161	−0.059	0.228	−0.008
sf-2	$n_{N3}-\sigma^*_{Se1-C2}$	12.87	0.94	0.098	1.965	0.036	0.049	−0.127	0.230	−0.153
sf-3	$n_{N3}-\sigma^*_{Se1-C2}$	3.20	0.94	0.049	1.971	0.037	0.109	−0.163	0.213	−0.159

[a] In kcal/mol. [b] In au.

the decrease in the electron density on the nitrogen lone pair in **f-1** (1.802), **tf-1** (1.740), and **sf-1** (1.723) and the increase in the second-order energy $E^{(2)}$ due to $n_N \rightarrow \pi^*_{C-X}$ bond delocalization in **f-1** (89.05), **tf-1** (111.2), and **sf-1** (120.4 kcal/mol). The trends in the elongation of the C−N bond length and the contraction in the C−X bond length (Table 1) also support the above arguments. Careful analysis of NBO data indicates that the increase in the delocalization as we move down the period is mainly attributable to the decrease in the energy difference between the energies of the N lone pair and the π^* orbital of C−X bond: 0.59 (**f-1**), 0.47 (**tf-1**), and 0.45 kcal/mol (**sf-1**). It is well established that the second-order interaction between any two orbitals increases with a decrease in the energy difference between them.[19] On the other hand, the electronegativity of X strongly influences the $n_N \rightarrow \sigma^*_{C-X}$ negative hyperconjugative interaction. Hence, in **f-2** this interaction is much stronger than in **tf-2**. The increase in the $p\pi-p\pi$ delocalization (in **f-1** < **tf-1** < **sf-1**) and decrease in the anomeric π interaction (in **f-2** > **tf-2** > **sf-2**) compliment each other in increasing the C−N rotational barrier in **tf-1** relative to **f-1**. In selenoformamide, the ΔE between the N lone pair and π^* of C−Se is small and hence the N lone pair delocalization is strong relative to thioformamide and formamide.

Ureas. The electronic structure of urea[20] has been studied extensively earlier but much less attention has been paid on the studies on thiourea[20] and selenourea.[21] Roberts and co-workers showed that the C—N rotational barrier in urea (11.0 kcal/mol) is smaller than that in thiourea (13.5 kcal/mol) and the increase in the C—N rotational barrier due to solvent interactions is stronger in thiourea.[20a]In this section, the electronic structures of urea, thiourea, and selenourea are compared. Figure 3 shows the various structures on the PE surfaces of **u-1**, **tu-1**, and **su-1**. The C—N rotational barriers in **u-1**, **tu-1**, and **su-1** are 7.52, 8.81, and 9.44 kcal/mol respectively at G2 level. The C—N rotational barrier in **su-1** is larger than that of **u-1** and **tu-1** at all levels of theoretical calculations. Similarly, the N-planarization energy in **u-1** (i.e. ΔE between **u-1** and **u-2**) (0.24 kcal/mol) is much larger than that in **tu-1** (0.15 kcal/mol) and **su-1** (0.16 kcal/mol). The C—N bond lengths (Figure 3) in these systems at MP2(full)/6-31+G* decrease in the order **u-1** (1.388 Å) > **tu-1** (1.374 Å) > **su-1** (1.367 Å), and the pyramidalization (taken as a measure of deviation of sum of angles from 360.0°) around N decrease in the same order **u-1** (16.7°), **tu-1** (12.9°), and **su-1** (9.9°). Elongation in the C—N bond length and the contraction in the C—X bond length during C—N rotation also (Table 1) follow similar trends that indicate an increase in the X—C—N delocalization as we go down the group. The atomic charges calculated using the NPA method (Table 7) clearly indicate strong polarization in the C—O bond in urea, which gets reduced in thiourea and further reduced in selenourea. These data support the arguments given by Wiberg and co-workers that the contribution of the resonance structure (**3**) increases at the expense of the dipolar structure (**2**) rather than of the canonical C═O structure (**1**) for the overall character of the "resonance hybrid" in amide bonds.

There is a strong $n_N \rightarrow \pi^*_{C-X}$ delocalization in urea, thiourea, and selenourea as in the case of the corresponding amides. NBO analysis (Table 7) shows that the $n_N \rightarrow \pi^*_{C-X}$ delocalization increases in the order O < S < Se; this is responsible for the increasing C−N rotational barriers in the same order. The second-order energy $E^{(2)}$ associated with this delocalization in **u-1**, **tu-1**, and **su-1** according to MP2(full)/6-31+G* are 56.75, 73.52, and 83.60 kcal/mol. This is due to the decrease in the E_{ij} values in the same order **u-1** (0.65), **tu-1** (0.52), and **su-1** (0.49 au). Hence, the increasing N lone pair delocalization in urea < thiourea < selenourea is mainly due to the orbital interactions rather than electronegativity on X. These observations are further confirmed by the decrease in the lone pair electron density on N in the order **u-1** (1.869e) > **tu-1** (1.824e) > **su-1** (1.807e) and increase in the π^* C−X electron densities **u-1** (0.258e) < **tu-1** (0.346e) < **su-1** (0.378e). The C−N rotational transition state structures **u-5**, **tu-5**, and **su-5** are characterized by $n_N \rightarrow \sigma^*_{C-X}$ and $n_N \rightarrow \sigma^*_{C-N}$ negative hyperconjugative interactions which decrease with a decrease in the electronegativity of X. This also contributes to the increase in the C−N rotational barrier in the order O < S < Se, because the negative hyperconjugative interactions get reduced in the same order.

The above analysis on isocyanates, formamides, and ureas clearly indicates that the electron delocalizations increase in the

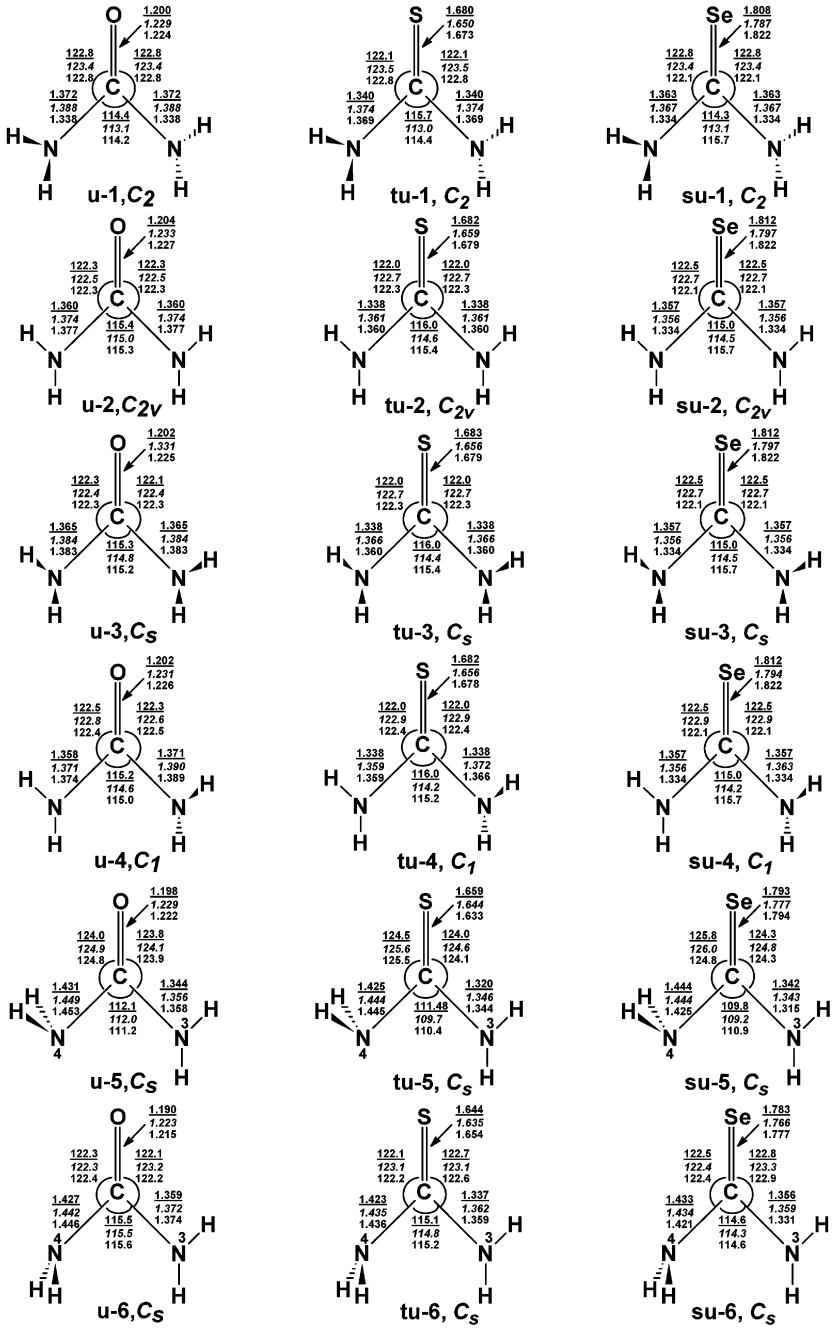

Figure 3. Different structures of urea, thiourea, and selenourea along with their important geometeric parameters at three levels (viz. HF/6-31+G*, MP(full)/6-31+G*, B3LYP/6-31+G*). Distances are in ångstroms and angles are in degrees.

order O < S < Se. Because the observed delocalization order does not follow the increasing electronegativity order, we can conclude that the electronegativity of X does not play an important role in the electron delocalization in these systems. The NBO analysis indicates that the π^* orbital plays an important role in increasing the electron delocalization. The strength of π^* interaction mainly depends on the antibonding overlap between the p atomic orbitals involved. The antibonding overlap in the C═X bond in X═CRNH$_2$ mainly depends on the p orbital coefficients on C and X in the π^* orbital and the distance between C and X. When the electronegativity on X is high, the p coefficient on X is low and hence the π^* strength is low. As the electronegativity on X decreases, the p orbital coefficients in the π^* orbital becomes equal and increase the energy of π^* orbitals. This should have decreased the π delocalization. However, with the increase in the *n* value, the 2p−np antibonding overlap decreases (n is 2, 3, and 4 for O, S, and Se, respectively) in addition, the C═X bond length increases with the size of X, decreasing the π^* strength. As a result, the strength of the antibonding interactions causes a decrease of the energy of the π^* orbital and a decrease in the energy difference (ΔE) between the N-lone pair and the π^*_{C-X} orbital. As ΔE decreases, charge transfer from the lone pair to the π^* orbital increases and hence the charge transfer to X increases, as observed by Wiberg et al.[3] as well as Lauvergnat and Hiberty et al.[5] Hence, it can be concluded that orbital interactions rather than the electronegativity play an important role in deciding electron delocalization.

The results discussed in the previous sections indicate that the orbital interactions rather than electronegativity of X play an important role in explaining the resonance phenomenon. This can be verified by studying the orbital interaction vs delocalization in X═C(H)NH$_2$ (where X = CH$_2$, SiH$_2$, NH, PH, AsH; R = H, NH$_2$) and compare with the above study. Wiberg et al.

TABLE 6: Relative Energies (kcal/mol, ZPE Corrected Values) of Various Structures of Urea (u), Thiourea (tu), and Selenourea (su) Obtained Using Different Theoretical Methods

structure	HF/6-31+G*	MP2/6-31+G*	MP2(full)/6-31+G*	B3LYP/6-31+G*	B3PW91/6-31+G*	G2
u-1	0.0	0.0	0.0	0.0	0.0	0.0
u-2	2.46	4.04	3.89	2.61	2.58	0.24
u-3	1.97	1.77	1.77	1.63	1.72	0.08
u-4	1.74	2.50	2.42	1.66	1.71	0.00
u-5	9.33	9.35	9.29	8.84	8.84	7.52
u-6	16.51	16.57	16.56	15.74	15.81	12.04
tu-1	0.0	0.0	0.0	0.0	0.0	0.0
tu-2	0.25	2.78	2.59	1.42	1.39	0.16
tu-3		1.81	1.88			0.15
tu-4		1.89	1.79	1.16	1.17	0.00
tu-5	10.10	9.02	8.96	9.21	9.25	8.81
tu-6	19.04	17.45	17.30	17.43	17.64	14.51
su-1		0.0	0.0	0.0	0.0	0.0
su-2	0.0	1.92	1.52	0.52	0.49	0.16
su-3		1.85	1.52			0.16
su-4		1.42	1.28			0.00
su-5	11.26	8.87	8.79	9.08	9.09	9.44
su-6	20.83	17.71	17.63	17.68	17.85	15.40

TABLE 7: NBO Analysis of Urea (u), Thiourea (tu), and Selenourea (su) at the MP2(full)/6-31+G* Level

		second-order interaction			occupancy	charges			
compound	interaction	$E^{(2)}$ [a]	$E_j - E_i$ [b]	$F_{i,j}$ [b]	$\rho_{n(N)}$	X	C	N^3H_2	N^4H_2
u-1	$n_N-\pi^*_{O-C2}$	56.75	0.65	0.177	1.892	−0.753	0.971	−0.109	−0.109
u-5	$n_{N3}-\pi^*_{O-C2}$	94.91	0.58	0.168	1.790(N3)	−0.739	0.960	−0.054	−0.167
	$n_{N4}-\sigma^*_{O-C2}$	15.14	1.41	0.131	1.968(N4)				
	$n_{N4}-\sigma^*_{C2-N4}$	4.35	1.26	0.067					
tu-1	$n_N-\pi^*_{S-C2}$	73.52	0.52	0.182	1.824	−0.267	0.384	−0.059	−0.059
tu-5	$n_{N3}-\pi^*_{S-C2}$	122.09	0.46	0.213	1.720(N3)	−0.231	0.356	0.010	−0.135
	$n_{N4}-\sigma^*_{S-C2}$	11.70	1.06	0.100	1.965(N4)				
	$n_{N4}-\sigma^*_{C2-N3}$	6.63	1.25	0.082					
su-1	$n_N-\pi^*_{Se-C2}$	83.60	0.49	0.189	1.807	−0.247	0.350	−0.052	−0.052
su-2	$n_N-\pi^*_{Se-C2}$	104.52	0.45	0.203	1.782	−0.284	0.362	−0.039	−0.039
su-5	$n_{N3}-\pi^*_{Se-C2}$	132.79	0.44	0.216	1.701(N3)	−0.198	0.317	0.017	−0.136
	$n_{N4}-\sigma^*_{Se-C2}$	11.51	0.94	0.093	1.963(N4)				
	$n_{N4}-\sigma^*_{C2-N3}$	7.03	1.25	0.084					
su-6	$n_{N3}-\pi^*_{Se-C2}$	113.28	0.46	0.204	1.742(N3)	−0.119	0.300	−0.001	−0.150
	$n_{N4}-\sigma^*_{Se-C2}$	2.33	0.92	0.041	1.964(N4)				
	$n_{N4}-\sigma^*_{C2-N4}$	14.10	1.19	0.116					

[a] In kcal/mol. [b] In au.

SCHEME 2: Schematic Diagram Showing the Second-Order Interaction between n_N and π^*_{C-X}, Which Indicates That the $n_N \rightarrow \pi^*_{C-Se}$ Delocalization Should Be Maximum because ΔE between n_N and π^*_{C-Se} Is Smallest

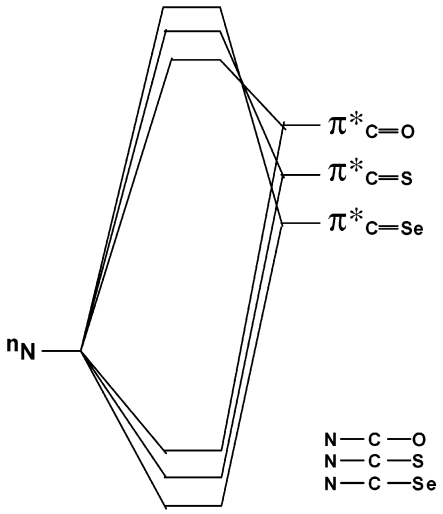

have showed that the C—N rotational barrier in vinylamine, **v-1**, methanimidamide **m-1**, and formamide **f-1**, increase in the order **v-1** < **m-1** < **f-1**, indicating a stronger delocalization with an increase in the electronegativity of X.[15b] We have performed

TABLE 8: NBO Analysis Corresponding to the $n_N \rightarrow \pi^*_{C-X}$ Interaction and C—N Rotational Barriers in Compounds with General Formulas X=C(H)-NH_2 and X= $C(NH_2)_2$ Using MP2 (full)/6-31+G* Optimized Parameters

X	ΔE [b]	$E_i - E_j$ [c]	F_{ij} [c]	rotational barrier [bd]
		X=$CHNH_2$		
CH_2	16.52	0.86	0.107	7.07
NH	19.97	1.09	0.119	11.02
O	89.05	0.59	0.205	17.33
PH	55.41	0.59	0.161	12.22
S	111.2	0.47	0.205	19.06
AsH	86.27	0.48	0.182	13.37
Se	120.4	0.45	0.208	20.89
		X=$C(NH_2)_2$		
CH_2	33.48	0.68	0.138	5.84
NH	45.99	0.68	0.162	7.08
O	56.75	0.65	0.177	8.40
PH	55.87	0.55	0.162	7.51
S	73.52	0.52	0.182	8.58
AsH	57.62	0.53	0.161	7.34
Se	83.60	0.49	0.189	8.69

[a] X=SiH_2, GeH_2 systems cannot be considered in this series because of their tendency to exist in divalent state. [b] In kcal/mol. [c] In atomic units. [d] MP2(full)/6-31+G* estimates.

NBO analysis on a series of systems (Table 8) using the MP2-(full)/6-31+G* optimized geometeries. The second-order energy $E^{(2)}$ due to $n_N \rightarrow \pi^*_{C-X}$ electron delocalization increases in the order **v-1** (16.52) < **m-1** (25.81) < **f-1** (89.09 kcal/mol),

SCHEME 3

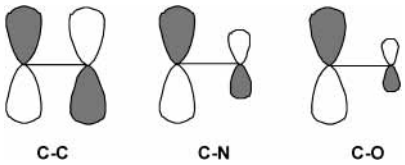

confirming the expectations. The ΔE between the interacting orbitals in these systems decrease in the same order **v-1** (0.86) > **m-1** (0.83) > **f-1** (0.59 au), this can be rationalized in the following way. In the π^* orbital of any C═X bond, the contribution from X is relatively smaller and hence there is antibonding overlap between the two p orbitals in the π^* orbital. The antibonding interaction in the C═O π^* orbital of formamide is weaker than that of the C═N π^* orbital of methanimidamide which is further weaker than the C═C π^* orbital in vinylamine because of reducing pπ−pπ^* overlap (Scheme 3). This is mainly due to the size of the p orbital on an X in the π^* orbital, which increases with the electronegativity along a row; the change in the size of X and the C−X bond length are much smaller in this case. This leads to a decrease in the ΔE between the n_N orbital and π^*_{C-X} orbital in the order **v-1** > **m-1** > **f-1**. The Fock matrix element between the interacting orbitals also increases as represented by an increase in the F_{ij} values 0.107, 0.132, and 0.205 au, respectively, for **v-1**, **tf-1**, and **f-1**. This also causes an increase in the energy of second-order interaction because $E^{(2)}$ is directly proportional to the square of F_{ij}. A similar trend is observed along the second (X = PH, S) and third (X = AsH, Se) rows also. The NBO data in Table 8 clearly indicates that along the row as well as the column in the periodic table, the extent of electron delocalization in X═CR(NH_2) systems follows the trend of ΔE between C═X π^* and the lone pair on N; i.e., with the decrease in ΔE the electron delocalization increases. This analysis indicates that the resonance in these systems depends mainly on the orbital interactions, which in turn depend on the size of the p atomic orbital on the X in the π^* MO of the system and hence the C−X polarization. Electronegativity of X and the size of the atom play an indirect role in deciding the extent of electron delocalization.

Conclusions

Ab initio MO and density functional calculations using high level methods indicate that C−N partial double bond character increases in formamides and ureas in the order O < S < Se. This is supported by the C−N rotational barriers, N-inversion barriers, charge distributions, extent of second-order interactions ($E^{(2)}$), electron occupancies of lone pair on nitrogen and the π^* C═X bonds, etc. Similarly, in the case of isocyanates also the electron delocalization has been shown to increase in the order O < S < Se. The trends in the electron delocalization cannot be explained on the basis of electronegativity of X. NBO analysis shows that the trends can be explained on the basis of the orbital interactions; i.e., the smaller the energy difference between the orbitals involved in the second-order delocalization, the greater is the resonance. This observation has been confirmed by the studies on the systems with X═CR−NH_2, (X = CH_2, NH, O, SiH_2, PH, S, AsH, Se; R = H, NH_2).

Acknowledgment. We thank Department of Science and Technology, New Delhi, for financial support.

Supporting Information Available: Tables S1−S3 containing the absolute energies of different systems. This material is available free of charge via the Internet at http://pubs.acs.org.

Note Added after ASAP Posting

This article was posted ASAP on 2/6/2003. In paragraph 1 of the Results and Discussion, isocyanete was changed to isocyanate. In paragraph 4 of the same section, C═N was changed to C−N throughout the paragraph. In Tables 3, 5, and 7, the alignment of "second-order interactions" was adjusted. A revised version was posted on 2/11/2003.

References and Notes

(1) (a) Pauling, L. *The Nature of Chemical Bond*,;Cornell University Press: Ithaca, NY, 1960. (b) Wheland, G. W. *Resonance in Organic Chemistry*; Wiley: New York, 1995.

(2) (a) Laidig, K. E.; Cameron, L. M. *J. Am. Chem. Soc.* **1996**, *118*, 1737. (b) Wiberg, K. B.; Laidig. K. E. *J. Am. Chem. Soc.* **1987**, *109*, 5935. (c) Wiberg, K. B.; Breneman, C. M. *J. Am. Chem. Soc.* **1992**, *114*, 831.

(3) (a) Wiberg, K. B.; Rush, D. J. *J. Am. Chem. Soc.* **2001**, *123*, 2038. (b) Wiberg, K. B.; Rablen, P. R. *J. Am. Chem. Soc.* **1995**, *117*, 2201. (c) Wiberg, K. B.; Breneman, C. M. *J. Am. Chem. Soc.* **1992**, *114*, 831. (d) Wiberg, K. B.; Breneman, C. M.; Lepage, T. J. *J. Am. Chem. Soc.* **1990**, *112*, 61. (e) Wiberg, K. B. In *The Amide Link*; Greenberg, A., Breneman, C. M., Liebman, J. F., Ed; Wiley: New York, 2000; p 41. (f) Wiberg, K. B.; Hadad, C. M.; Rablen, P. R.; Cioslowsk, J. *J. Am Chem. Soc.* **1992**, *114*, 8644. (g) Wiberg, K. B.; Rablen, P. R. *J. Am Chem. Soc.* **1993**, *115*, 9234. (h) Wiberg, K. B.; Ochterski, J.; Streitwieser, A. *J. Am Chem. Soc.* **1996**, *118*, 829. (i) Wiberg, K. B.; Rush, D. J. *J. Org. Chem.* **2002**, 67, 826.

(4) Glendening, E. D.; Hrabal, J. A., II. *J. Am. Chem. Soc.* **1997**, *119*, 12940.

(5) Lauvergnat, D.; Hiberty, P. C. *J. Am. Chem. Soc.* **1997**, *119*, 9478.

(6) (a) Hehre, W. J.; Radom, L.; Schleyer, P. v. R.; Pople, J. A. *Ab Initio Molecular Orbital Theory*; Wiley: New York, 1986. (b) Foresman, J. B.; Frisch, E. *Exploring Chemistry with Electronic Structure Methods*, 2nd ed.; Gaussian Inc., Pittsburgh, PA, 1996.

(7) (a) Parr, R. G.; Yang, W. *Density-Functional Theory of Atoms and Molecules*; Oxford University Press: New York, 1989. (b) Bartolotti, L. J.; Fluchick, K. In *Reviews in Computational Chemistry*; Lipkowitz, K. B., Boyd, D. B., Eds.; VCH Publishers: New York, 1996; Vol. 7, p 187.

(8) Frisch, M. J.; Trucks, G. W.; Schlegel, H. B.; Scuseria, G. E.; Robb, M. A.; Cheeseman, J. R.; Zakrzewski, V. G.; Montgomery, J. A., Jr.; Stratmann, R. E.; Burant, J. C.; Dapprich, S.; Millam, J. M.; Daniels, A. D.; Kudin, K. N.; Strain, M. C.; Farkas, O.; Tomasi, J.; Barone, V.; Cossi, M.; Cammi, R.; Mennucci, B.; Pomelli, C.; Adamo, C.; Clifford, S.; Ochterski, J.; Petersson, G. A.; Ayala, P. Y.; Cui, Q.; Morokuma, K.; Malick, D. K.; Rabuck, A. D.; Raghavachari, K.; Foresman, J. B.; Cioslowski, J.; Ortiz, J. V.; Baboul, A. G.; Stefanov, B. B.; Liu, G.; Liashenko, A.; Piskorz, P.; Komaromi, I.; Gomperts, R.; Martin, R. L.; Fox, D. J.; Keith, T.; Al-Laham, M. A.; Peng, C. Y.; Nanayakkara, A.; Gonzalez, C.; Challacombe, M.; Gill, P. M. W.; Johnson, B.; Chen, W.; Wong, M. W.; Andres, J. L.; Gonzalez, C.; Head-Gordon, M.; Replogle, E. S.; and. Pople, J. A. *Gaussian 98*, revision A.7; Gaussian, Inc.: Pittsburgh, PA, 1998.

(9) Krishan, R.; Frisch, M. J.; Pople, J. A. *J. Chem. Phys.* **1980**, *72*, 4244.

(10) (a) Becke, A. D. *J. Chem. Phys.* **1993**, *98*, 5648. (b) Lee, C.; Yang, W.; Parr, R. G. *Phys. Rev. B* **1980**, *37*, 785. (c) Perdew, J. P.; Wang, Y. *Phys. Rev. B* **1992**, *45*, 13244.

(11) Salter, E. A.; Trucks, G. W.; Bartlett, R. J. *J. Chem. Phys.* **1989**, 90, 1752.

(12) Scott, A. P.; Radom, L. *J. Phys. Chem.* **1996**, *100*, 16502.

(13) Curtiss, L. A.; Raghavachari, K.; Trucks, G. W.; Pople. J. A. *J. Chem. Phys.* **1991**, *94*, 7221.

(14) (a) Reed, A. E.; Weinstock, R. B.; Wienhold, F. *J. Chem. Phys.* **1985**, *83*, 735. (b) Reed, A. E.; Curtiss, L. A.; Wienhold, F. *Chem. Rev.* **1988**, *88*, 899.

(15) (a) Sakaizumi, T.; Yasukawa, A.; Miyamoto, H.; Ohashi, O.; Yamaguchi. *Bull. Chem. Soc. Jpn.* **1986**, *59*, 1614. (b) Lett, R. G.; Flygare, W. H. *J. Chem. Phys.* **1967**, *47*, 4730. (c) Kreglewski, M. *Chem. Phys. Lett.* **1984**, *112*, 275. (d) Koput. J. *J. Mol. Spectrosc.* **1984**, *106*, 12. (e) Landsberg, B. M. *Chem. Phys. Lett.* **1979**, *60*, 265. (f) Yamada, K.; Winnewisser, M.; Winnerwisser, G.; Szalanski, L. B.; Gerry, M. C. L. *J. Mol. Spectrosc.* **1980**, *79*, 295. (g) Yamada. K. *J. Mol. Spectrosc.* **1980**, *79*, 323. (h) The experimentally estimated N-inversion barrier in Me−N−C−Se is 0.71 kcal/mol. Koput, J.; Stroh, F.; Winnerwisser, M. *J. Mol. Spectrosc.* **1990**, *140*, 31.

(16) (a) Wolf, R.; Wong, M. W.; Kennard, C. H. L.; Wentrup. C. *J. Am. Chem. Soc.* **1995**, *117*, 6789. (b) Wolf, R.; Stadtmuller, V.; Wong, M. W.; Flammang, M. B.; Flammang, R.; Wentrup, C. *Chem. Eur. J.* **1996**, *2*, 1318.

(17) (a) Bharatam, P. V.; Uppal, P.; Bassi, P. S. *Chem. Phys Lett.* **1997**, *276*, 31. (b) Leszczynski, J.; Kwiatkowski, J. S.; Leszczynska, D. *J. Am. Chem. Soc.* **1992**, *114*, 10089.

(18) (a) Sandstrom, J. *J. Phys. Chem*. **1967**, *71*, 2318. (b) Neuman, R. C., Jr.; Young, L. B. *J. Phys. Chem*. **1965**, *69*, 2570. (c) Loewenstein, A.; Melera, A.; Ringy, P.; Walter, W. *J. Phys. Chem.* **1964**, *68*, 1597. (d) Stewart, W. E.; Siddali, T. H., III. *Chem. Reν.* **1970**, *70*, 517.

(19) Albright, T. A.; Burdett, J. K.; Whangbo, M.-H. *Orbital Interactions in Chemistry*; John Wiley & Sons: New York, 1985.

(20) (a) Haushalter, K. A.; Lau, J.; Roberts, J. D. *J. Am. Chem. Soc.* **1996**, *118*, 8891 and references therein. (b) Zhao, Y.; Katherine, R.; Tsai,H.; Roberts. J. D. *J. Phys. Chem.* **1993**, *97*, 2910. (c) Godfrey, P. D.; Brown, R. D.; Hunter. A. N. *J. Mol. Struct*. **1997**, *413*−*414*, 405. (d) Meier, R. J.; Coussens. B. *J. Mol. Struct. (THEOCHEM)*. **1992**, *253*, 25. (e) Galabov, B.; Iiieva, S.; Hadjieva, B.; Dudev, T. *J. Mol. Struct*. **1997**, *407*, 47. (f) Chamberss, C. C.; Archibong, E. F.; Jabalameli, A.; Sullivan, R. H.; Giesen, D. J.; Cramer, C. J.; Truhlar, D. G. *J. Mol. Struct*. **1998**, *425*, 61. (g) Dixon, D. A.; Matsuzawa, N. *J. Phys. Chem.* **1994**, *98*, 3967. (h) Kontoyianni, M.; Bowen, J. P. *J. Comput. Chem*. **1992**, *13*, 657. (i) Ha, T.-K.; Puebla, C. *Chem. Phys*. **1994**, *181*, 47. (j) Gobbi, A.; Frenking, G. *J. Am. Chem. Soc*. **1993**, *115*, 2362.

(21) (a) Koketsu, M.; Suzuki, N.; Ishihara, H. *J. Org. Chem*. **1999**, *64*, 6473. (b) Dianez, M. J.; Estrada, M. D.; Lopez-Castro, A. *Carbohydr. Res.* **1993**, *242*, 265. (c) Pathirana, H. M. K. K.; Weiss, T. J.; Reibenspies, J. H.; Zingaro, R. A.; Meyers, E. A. *Z. Kristallogr*. **1994**, *109*, 697. (d) Billing, D. J.; Boeyens, J. C. A.; Denner, L.; Hellyar, M. D.; Lai, L. L.; Matthee, A. J.; Reid, D. H. *Acta Crystallogr*. **1993**, *C47*, 2564. (e) Billing, D. J.; Ferg, E. E.; Lai, L. L.; Levedis, D. C.; Reid, D. H. *Acta Crystallogr.* **1993**, *C49*, 917. (f) Guzman, J. F. B.; Skrydstrup, T, Lopez-Castro, A.; Millan, J. D.; Estrada de Oye, M. D. *Carbohydr. Res.* **1992**, *237*, 303.